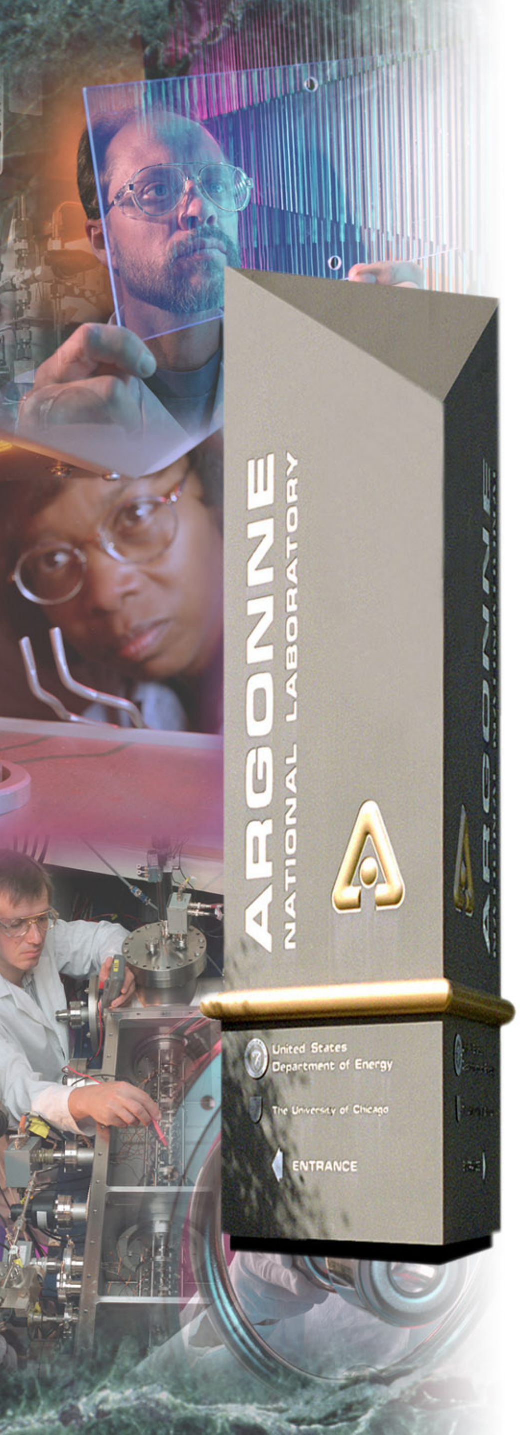

Universal Iterative Phasing Method for Near-Field and Far-Field Coherent Diffraction Imaging

Qun Shen (APS, ANL)
Xianghui Xiao (Cornell)

- ⇒ Imaging in different regimes
  - ❖ near-field phase contrast
  - ❖ in-line holography
  - ❖ coherent diffraction
- ⇒ Distorted object approach
  - ❖ Fresnel wave propagation by FFT
  - ❖ unified iterative phasing
- ⇒ Recent activities at APS
  - ❖ coherent imaging beamline
  - ❖ phase-sensitive topography
  - ❖ dose estimates & scaling with resolution
- ⇒ Summary

Office of Science
U.S. Department of Energy

A U.S. Department of Energy
Office of Science Laboratory
Operated by The University of Chicago

Different Regimes of X-ray Imaging

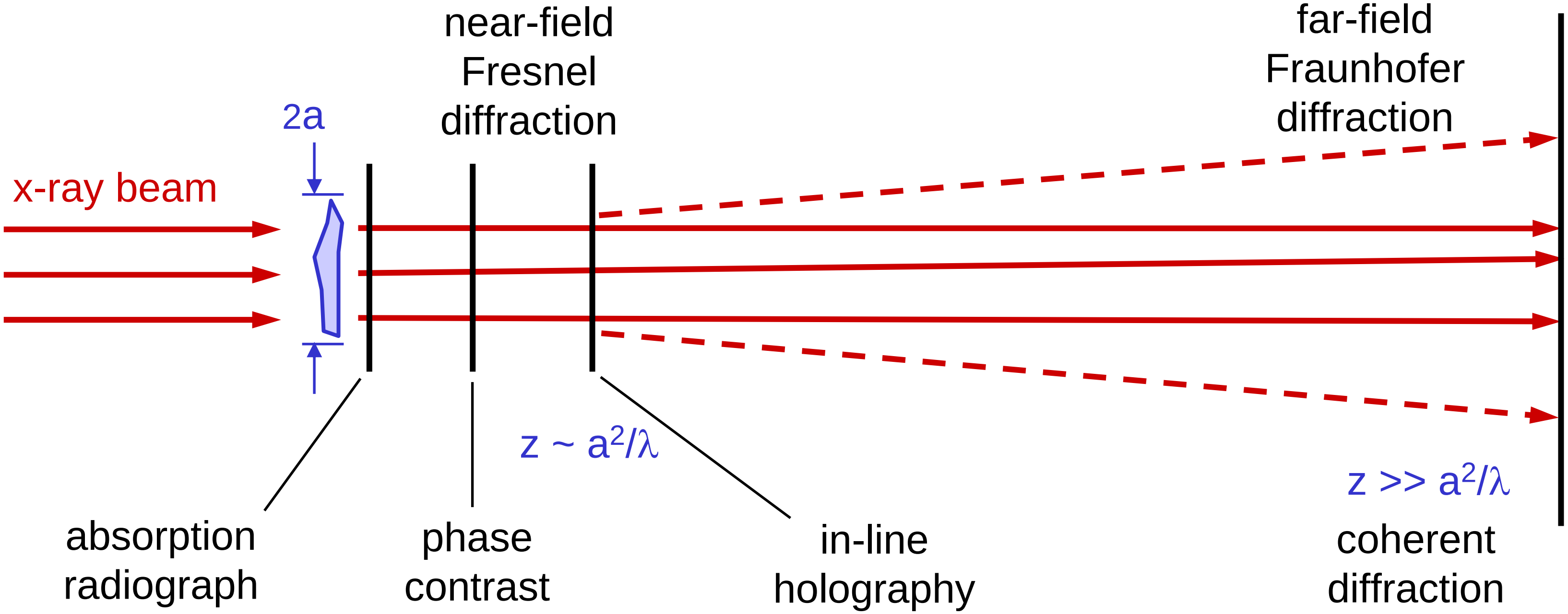

x-ray beam

2a

near-field
Fresnel
diffraction

far-field
Fraunhofer
diffraction

$z \sim a^2/\lambda$

$z >> a^2/\lambda$

absorption
radiograph

phase
contrast

in-line
holography

coherent
diffraction

Kagoshima et al.
JJAP (1999).

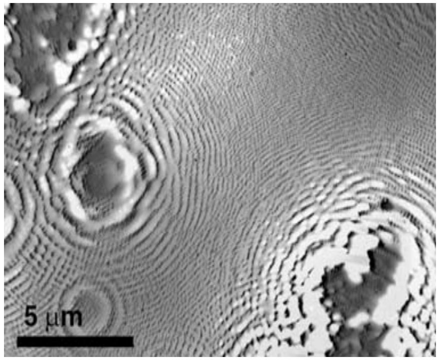

Jacobsen (2003).

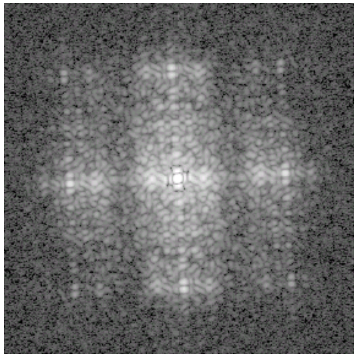

Miao et al.
Nature (1999).

Image Reconstruction in Different Regimes

⇒ Absorption regime
- ❖ straightforward, based on intensity attenuation
- ❖ 3D tomographic reconstruction

⇒ Phase contrast regime
- ❖ edge-enhanced shape recognition
- ❖ transport of intensity equation (TIE)
- ❖ holotomographic method based on Tolbot effect

⇒ In-line holographic regime
- ❖ holographic reconstruction
- ❖ twin-image problem

⇒ Far-field regime
- ❖ iterative phasing method
- ❖ Fourier transforms in real and reciprocal space
- ❖ requires oversampled diffraction pattern

→ **Unified Method ?**

Iterative Method in Far-field Diffraction

Gerchberg & Saxton, Optik 35, 237 (1972)

Fienup, Appl. Opt. 21, 2758 (1982)

$$\rho(x,y) \xleftrightarrow{\mathcal{F}} F(u,v) = |F(u,v)|\,\exp[i\phi(u,v)]$$

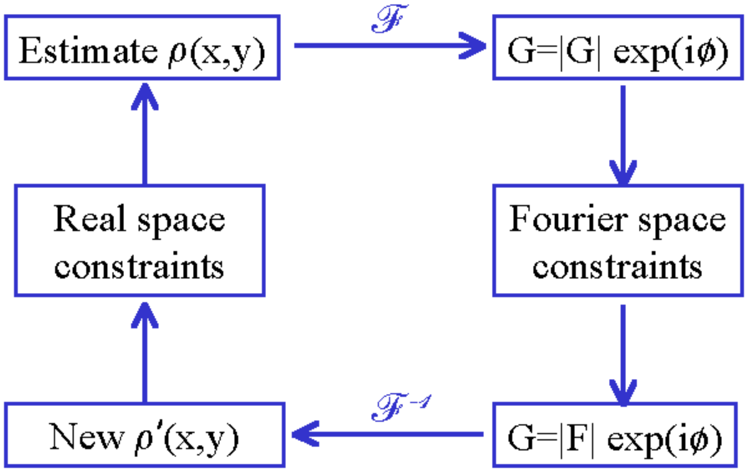

Estimate $\rho(x,y)$ $\xrightarrow{\mathcal{F}}$ $G=|G|\,\exp(i\phi)$

Fourier space constraints

$G=|F|\,\exp(i\phi)$ $\xrightarrow{\mathcal{F}^{-1}}$ New $\rho'(x,y)$

Real space constraints

Question: Can we extend FFT-based iterative algorithm to near-field ?

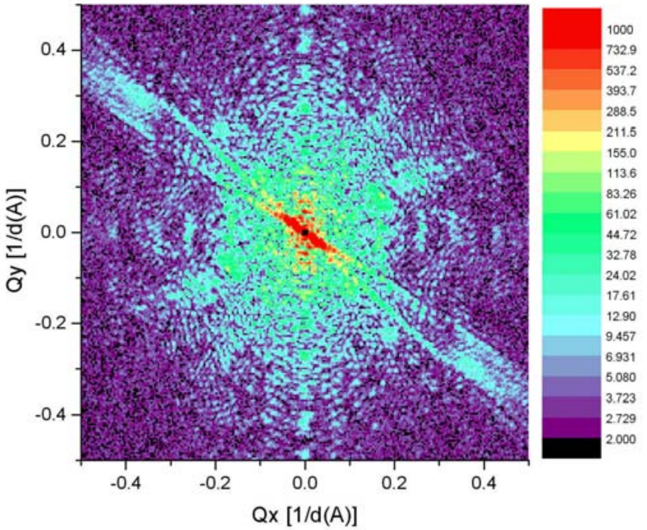

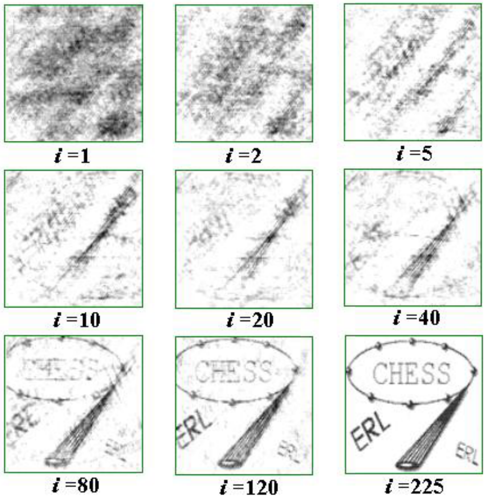

Elser, JOSA, A20, 40 (2003); Shen et al, JSR 11, 432 (2004)

Fresnel Wave Field Propagation

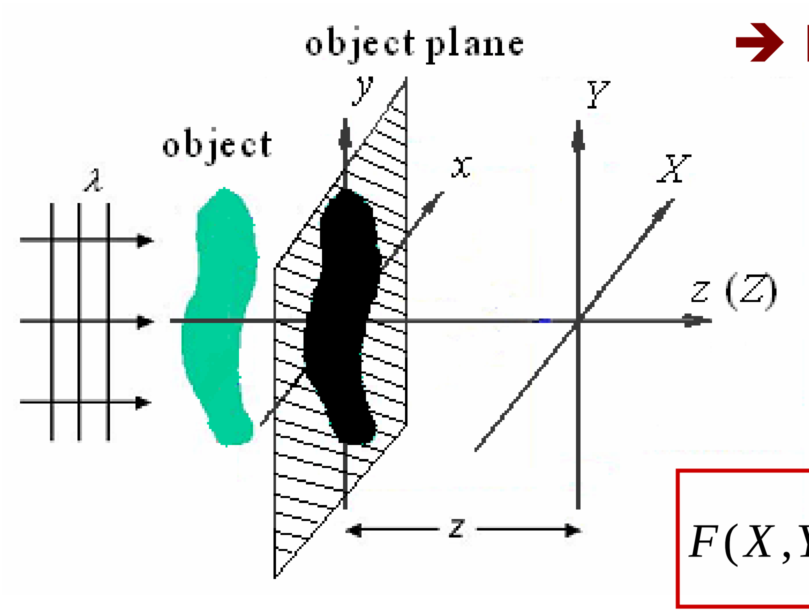

➔ Fresnel formula for wave propagation

$$\boxed{F(X,Y)=\frac{i}{\lambda}\iint u(x,y)\frac{e^{-ikr}}{r}dxdy}$$

$$r=[z^2+(X-x)^2+(Y-y)^2]^{1/2}$$

$$\approx\ z+[(X-x)^2+(Y-y)^2]/2z$$

$$\boxed{F(X,Y)=\frac{i\,e^{-ikR}}{\lambda R}\iint \underbrace{u(x,y)e^{-\frac{i\pi}{\lambda z}\left(x^2+y^2\right)}}_{}\,e^{-\frac{i2\pi}{\lambda z}(Xx+Yy)}dxdy}$$

$$R=(x^2+y^2+z^2)^{1/2}$$

➔ Wave-field in the object plane

$$u(x,y,0)=\exp(-ik\cdot\int_{-\infty}^{0}(\delta(x,y,z)-i\beta(x,y,z))dz)$$

$$u(x,y,0)=A\exp(-i\phi(x,y,0))=a(x,y,0)+ib(x,y,0)$$

$$\approx\exp(-ik\int_{-\infty}^{0}\delta(x,y,z)dz)\quad\text{(pure phase object)}$$

Van der Veen & Pfeiffer,
J. Phys.: Condens. Matter 16, 5003 (2004)

Distorted Object Approach

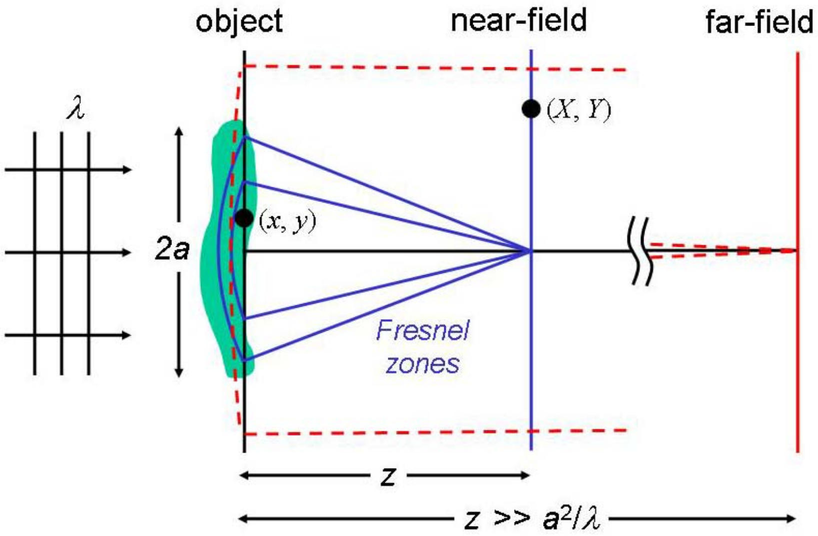

Phase-chirped distorted object:

$$\bar{u}(x,y) \equiv u(x,y)\,e^{-\frac{i\pi}{\lambda z}\left(x^2+y^2\right)}$$

$$F(X,Y) = \frac{i\,e^{-ikR}}{\lambda R}\iint \bar{u}(x,y)\,e^{-\frac{ik}{z}(Xx+Yy)}\,dxdy$$

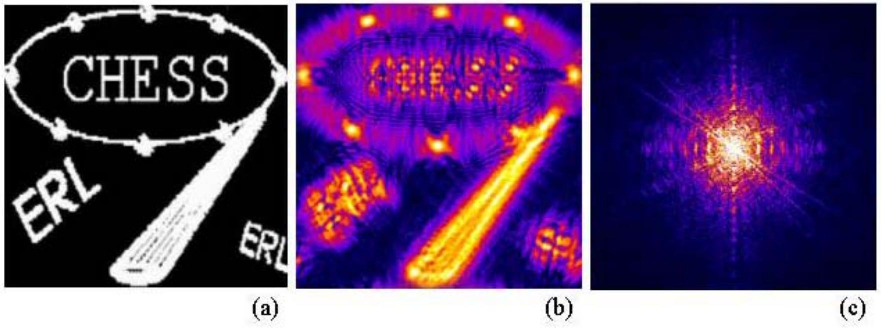

(a) (b) (c)

Fig.2: Simulated diffraction amplitudes |$F(X,Y)$|, of an amplitude object (a) of 10μm x 10μm, with λ = 1 Å x-rays, at image-to-object distance (b) z = 2mm and (c) z = ∞, using the unified distorted object approach (above) with N_z = 500 zones in (b) and N_z = 0 in (c). Notice that the diffraction pattern changes from noncentrosymmetric in the near-field (b) to centrosymmetric in the far-field (c).

⇒ Unified wave propagation method by Fourier transform

Momentum transfer: $(Q_x, Q_y) = (kX/z, kY/z)$

Number of Fresnel zones: $N_z = a^2/(\lambda z)$

Xiao & Shen, PRB, in press (July 2005)

Iterative Phasing with Distorted Object

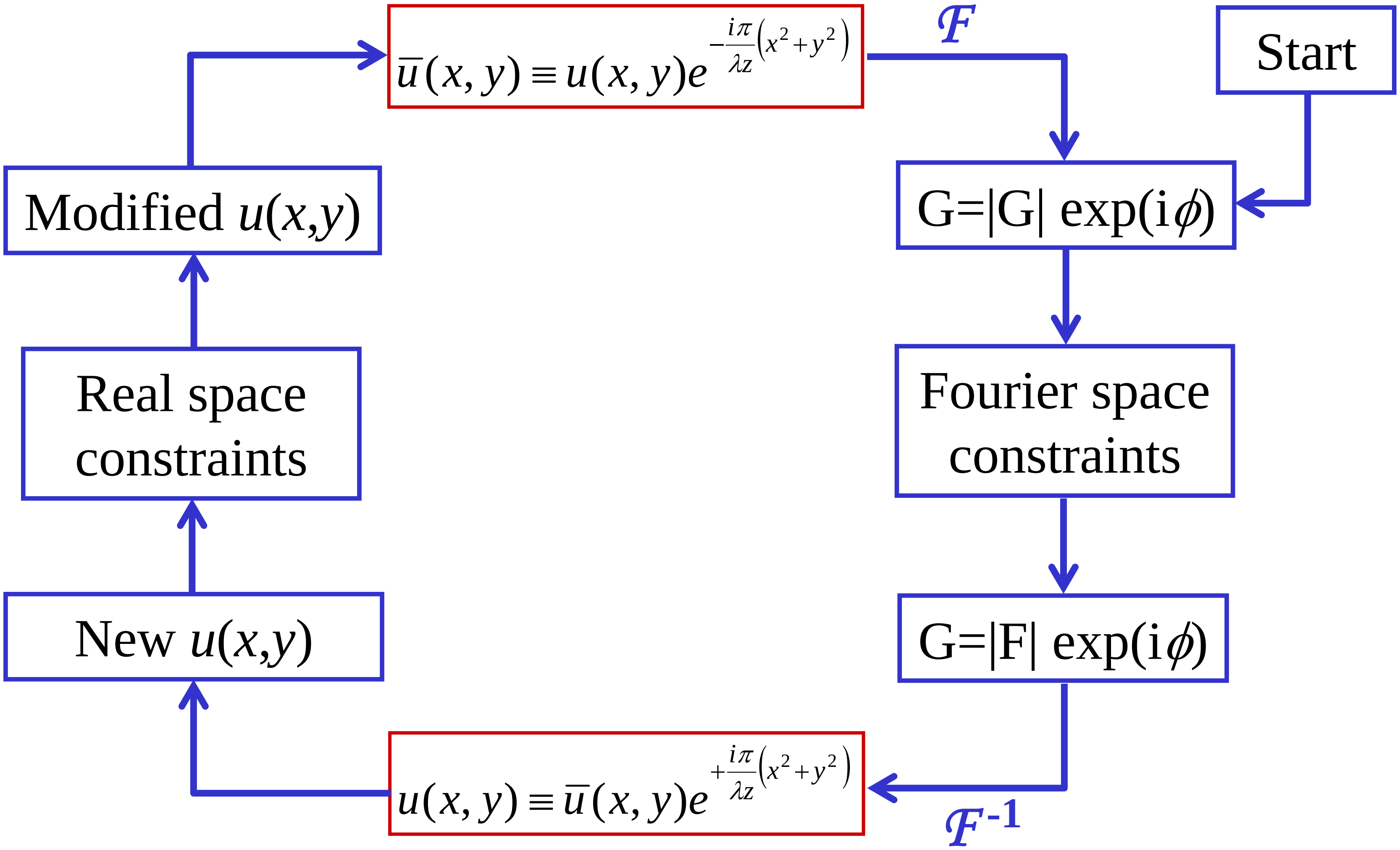

Start

G=|G| exp(iϕ)

Fourier space constraints

G=|F| exp(iϕ)

$\mathcal{F}^{-1}$

$$u(x,y) \equiv \bar{u}(x,y)\, e^{+\frac{i\pi}{\lambda z}\left(x^2+y^2\right)}$$

New $u(x,y)$

Real space constraints

Modified $u(x,y)$

$$\bar{u}(x,y) \equiv u(x,y)\, e^{-\frac{i\pi}{\lambda z}\left(x^2+y^2\right)}$$

$\mathcal{F}$

Oversampling @ 2x Nyquist f = Correct Sampling

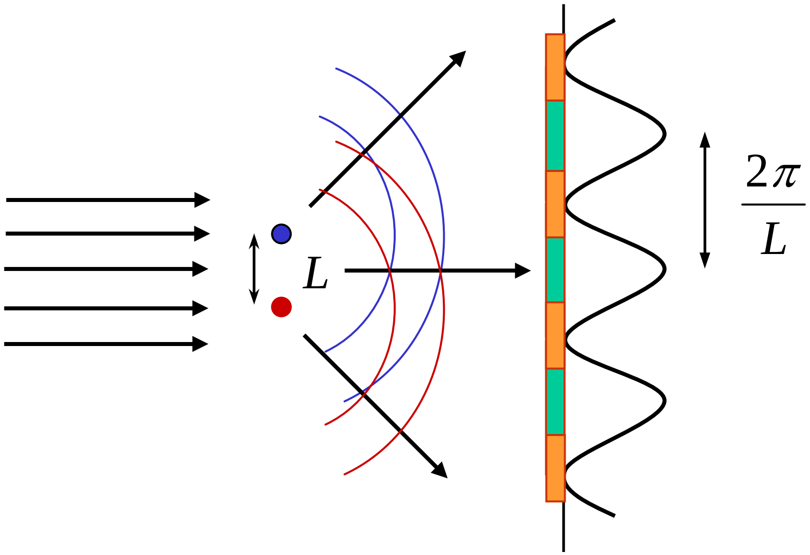

=> Sampling at frequency $2\pi/L$ in Fourier space is not fine enough to resolve interference fringes!

=> Additional measurements in-between $2\pi/L$ are necessary to tell us some interference is going on.

=> Minimum oversampling ratio is 2, regardless whether it is 1D, 2D or 3D.

$$\Delta Q_{\max}^{1\mathrm{D}} = \frac{2\pi}{L} \cdot \frac{1}{2} = \frac{\pi}{L}$$

$$\Delta Q_{\max}^{2\mathrm{D}} = \frac{2\pi}{L} \cdot \frac{1}{\sqrt{2}} = \frac{\sqrt{2}\pi}{L}$$

$$\Delta Q_{\max}^{3\mathrm{D}} = \frac{2\pi}{L} \cdot \frac{1}{\sqrt[3]{2}}$$

X-ray wavelength is λ, object's half width *a*, object-image distance *z*, and oversampling factor *O*, the pixel size of detector

$$\Delta X \le \frac{a}{2O \cdot N_z}, \qquad N_z = \frac{a^2}{\lambda \cdot z}$$

or $$\Delta X \le \frac{\lambda z}{O \cdot a}$$

Numerical Simulation Example

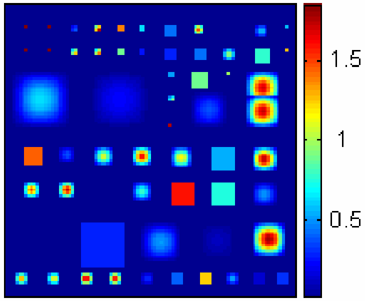

Material: Carbon; Object size: 10x10 micron; Maximum thickness ~10 μ m;

X-ray: 1Å; Maximum phase difference ~1.87rad; Absorption contrast~0.1%;

Oversampling factor: 2x2.

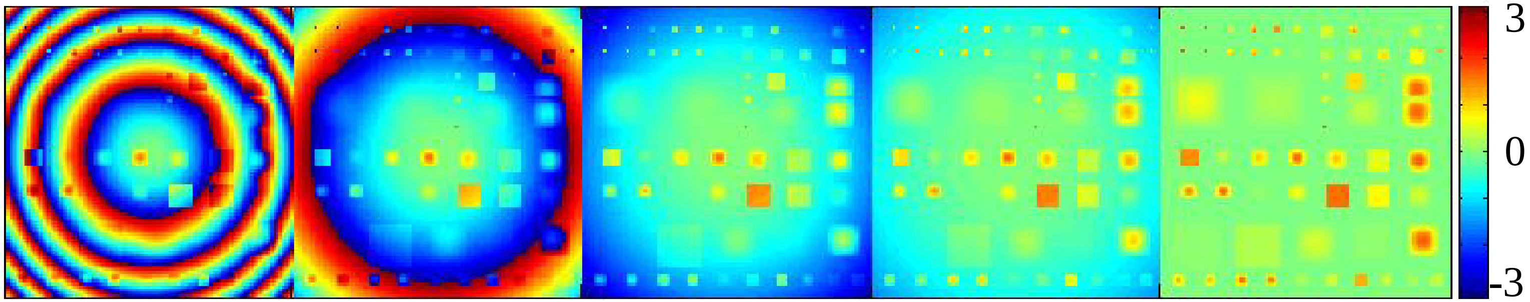

z = 5 cm $N_z = 5$ | z = 20cm $N_z = 1.25$ | z = 50cm $N_z = 0.5$ | z = 100cm $N_z = 0.25$ | $z = \infty$ $N_z = 0$

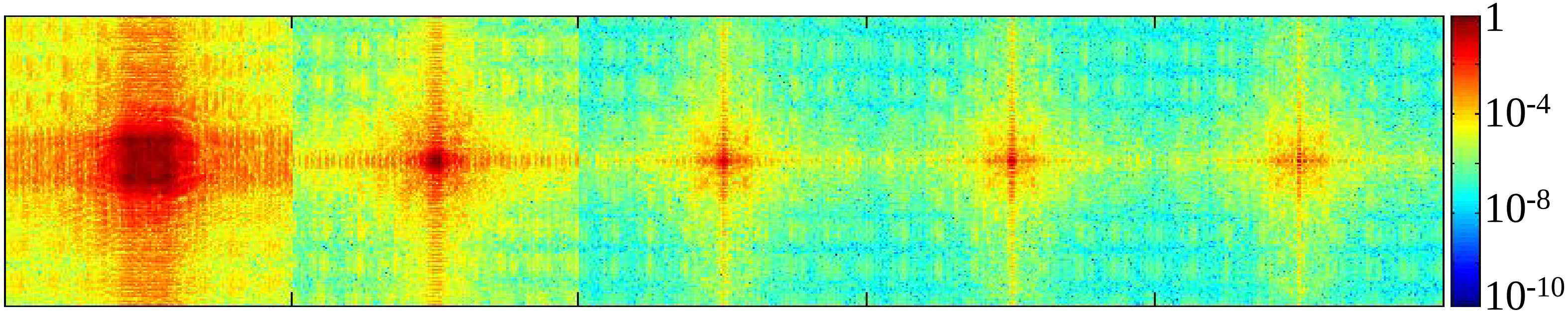

ΔX = 0.25 um | ΔX = 1 um | ΔX = 2.5 um | ΔX = 5 um | $\Delta X \propto z$

Phasing Results

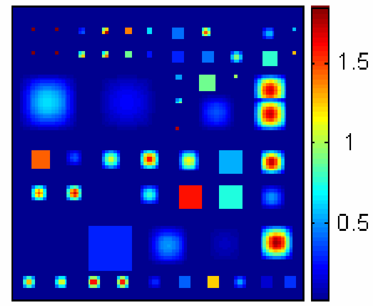

Xiao & Shen, PRB, in press (July 2005)

Twin image?

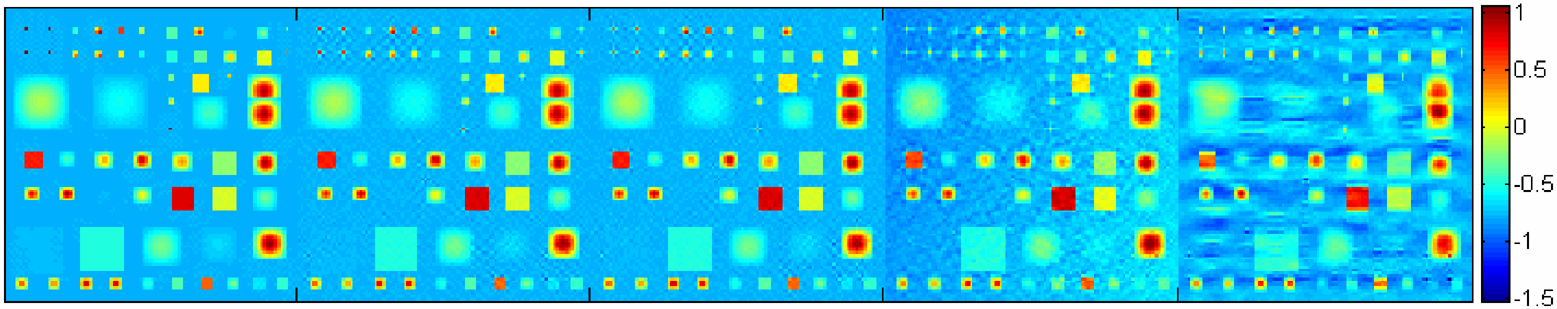

$z = 5\text{cm}$ $z = 20\text{cm}$ $z = 50\text{cm}$ $z = 100\text{cm}$ $z = \infty$

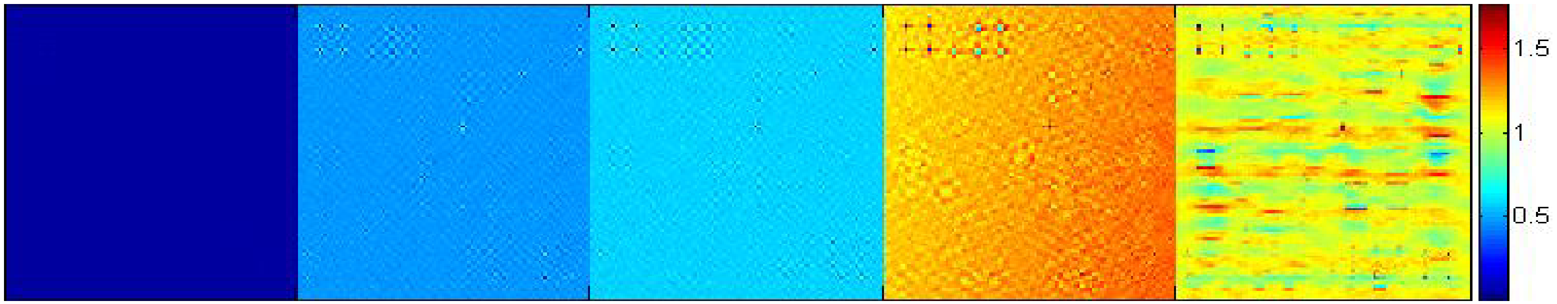

$R = 0.9998$ $R = 0.9954$ $R = 0.9943$ $R = 0.9639$ $R = 0.9248$

Comparisons with Far-field

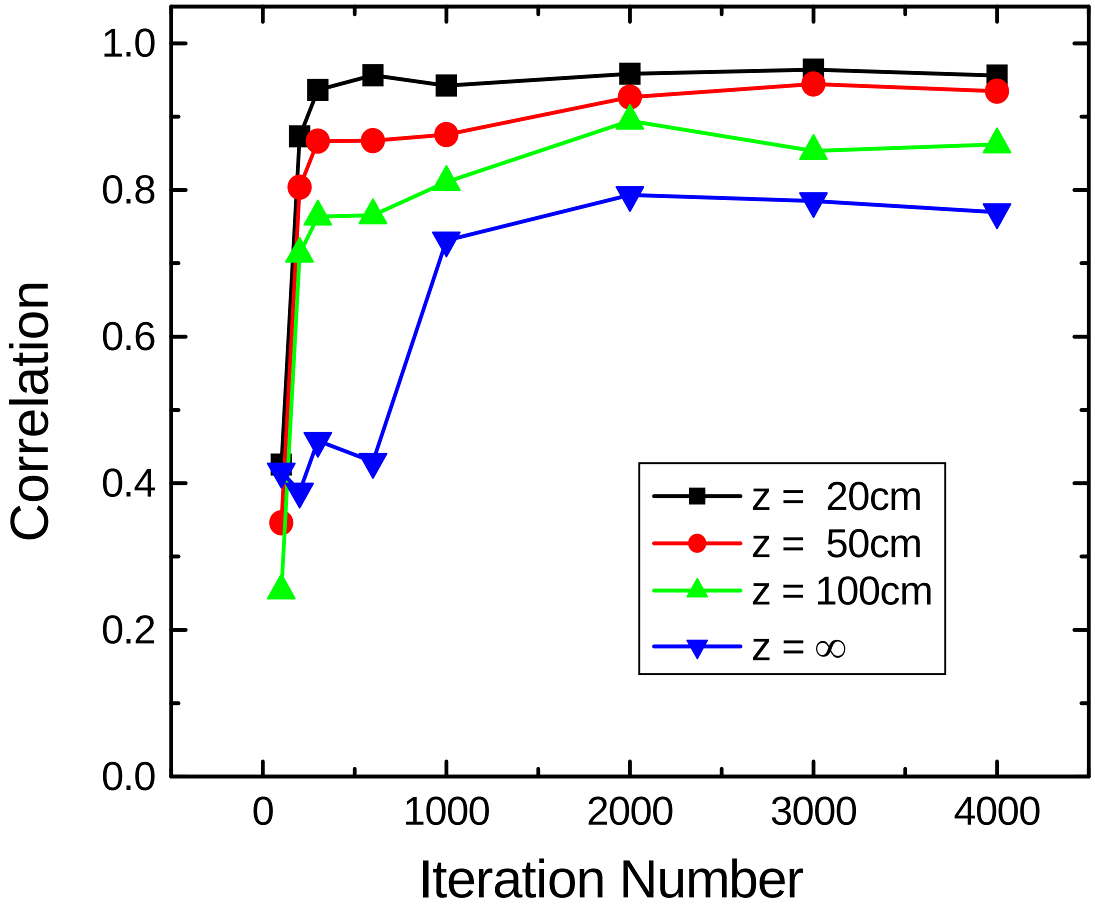

- Correlation coefficient between reconstructed phase map and the original phase map as a function of number of iterations in the iterative phase retrieval using the distorted object approach.
- Statistical Poisson noises are included in all diffraction patterns in these simulations.
- All these diffraction patterns are assumed to have the same total integrated intensity of 4.4x10^7 photons.
- Maximum intensity in the diffraction patterns are 7.6x10^5, 6.2x10^6, 8.8x10^6 and 1x10^7 photons, for z = 20cm, 50cm, 100cm, and far-field, respectively.

Distorted Object & Astigmatic Diffraction

K.A. Nugent et al, Acta Cryst. A61, 373-381, (2005)

$$U(X,Y)=\int_{-\infty}^{\infty}\int_{-\infty}^{\infty}u(x,y,0)\cdot\exp(i\frac{2\pi}{\lambda}\cdot\frac{q^2}{2R})\cdot\exp(i2\pi(\frac{x\cdot X}{\lambda\cdot z}+\frac{y\cdot Y}{\lambda\cdot z}))dxdy$$

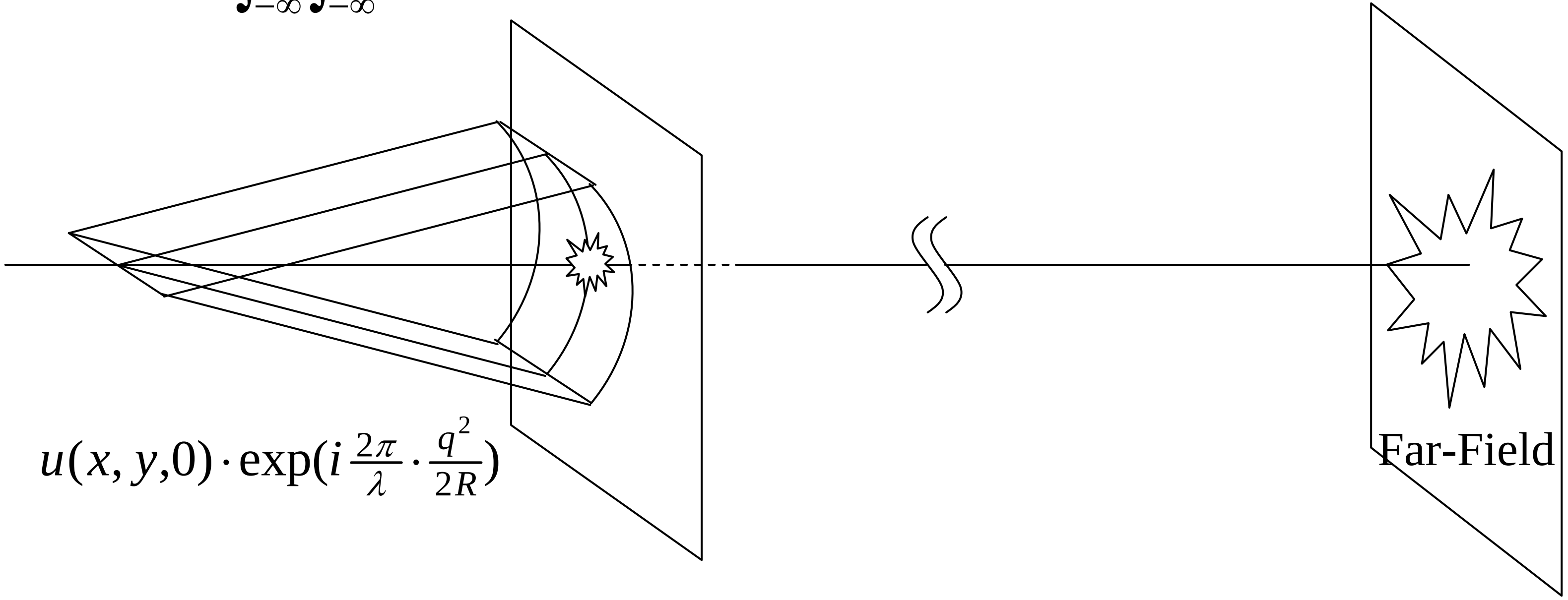

$$u(x,y,0)\cdot\exp(i\frac{2\pi}{\lambda}\cdot\frac{q^2}{2R})$$

Astigmatic diffraction (curved beam) method: create parabolic or spherical wave front with K-B mirror, FZP lens

Distorted object method: move detector a little bit closer to the sample comparing with conventional far-field imaging

Test Experiment at 32-ID-B

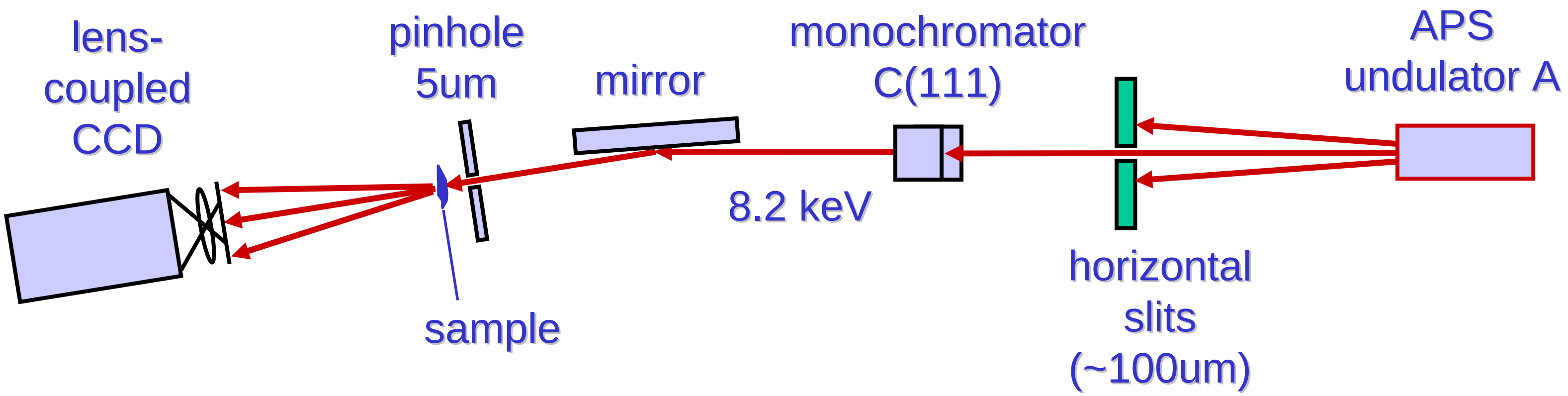

Dr. Xianghui Xiao (CHESS, Cornell University)

Specimen Used in Experiment

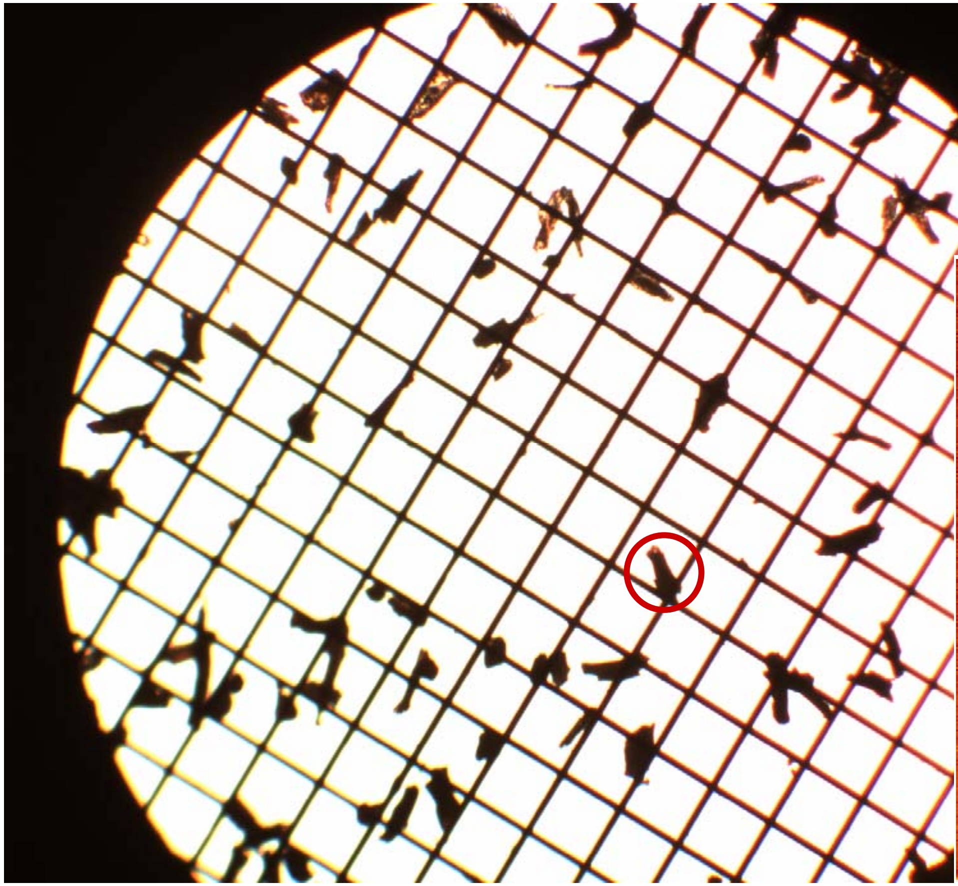

Specimen: cardiac myocytes
Brad Palmer (Univ. Vermont)

Differential phase contrast image with a configured detector (Chris Jacobsen)

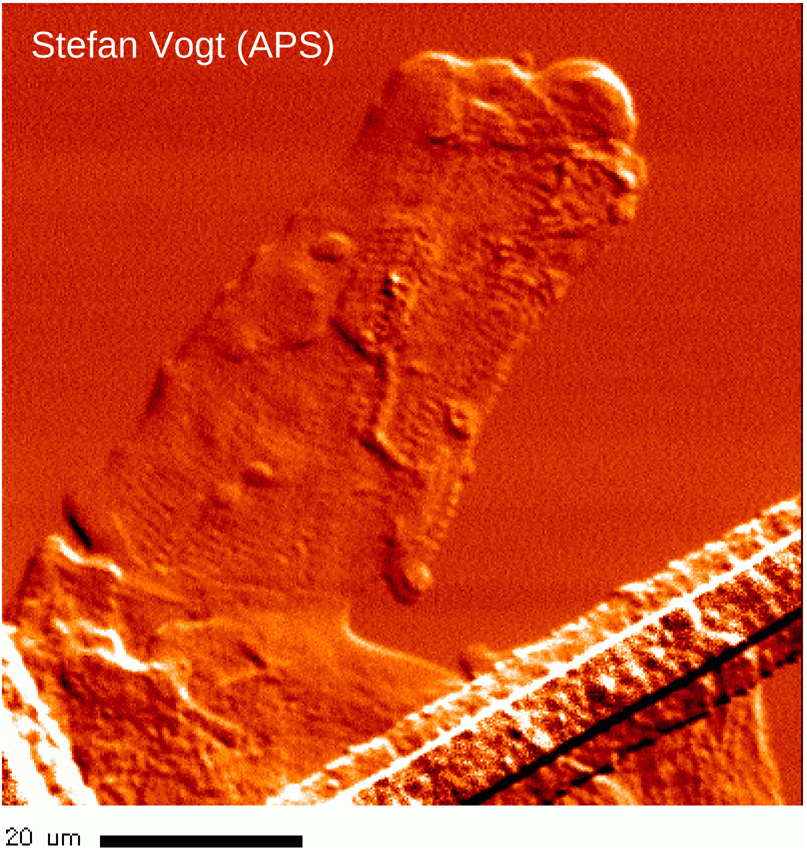

Preliminary Results on Myocytes

- Data obtained June 10-12, 2005
- Multiple images with different exposure times to avoid saturation (need stitching)

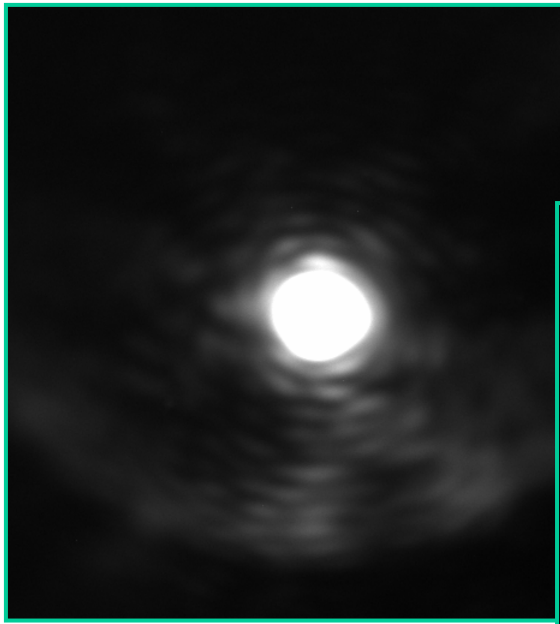

Z = 910 mm
$N_z = 0.045$, $\Delta X < 27um$
$\Delta x = 330nm$

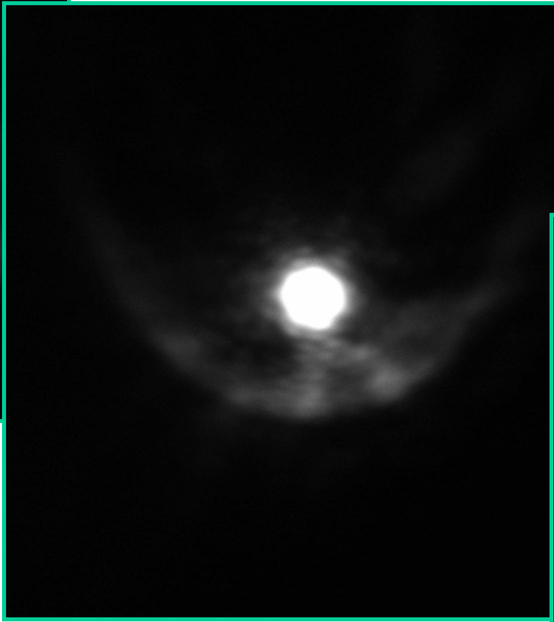

Z = 455 mm
$N_z = 0.09$, $\Delta X < 14um$
$\Delta x = 160nm$

Z = 277 mm
$N_z = 0.15$, $\Delta X < 8um$
$\Delta x = 100nm$

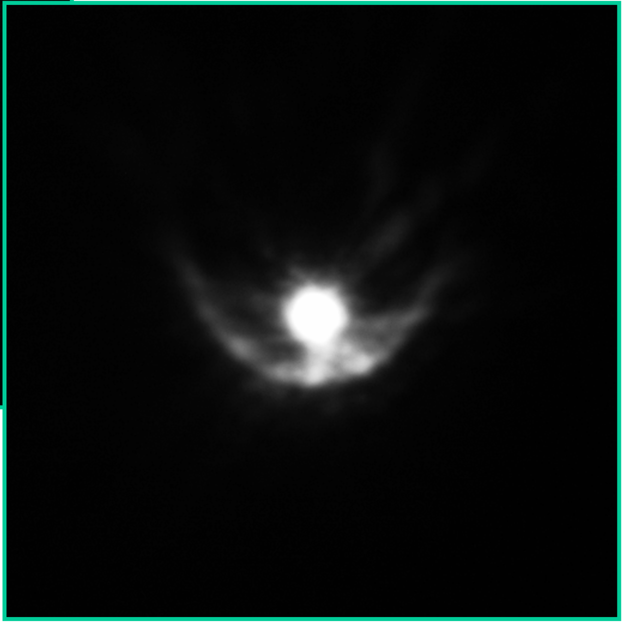

- Images at several z with $N_z = 0.045 – 0.45$
- Data processing in progress ….

Improving Experimental Setup

- Pinhole scattering ➔ need scatter shields
- Use multiple silicon nitride windows
- Need four independent x-y translations

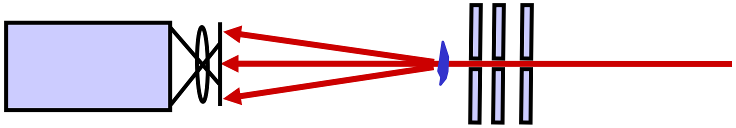

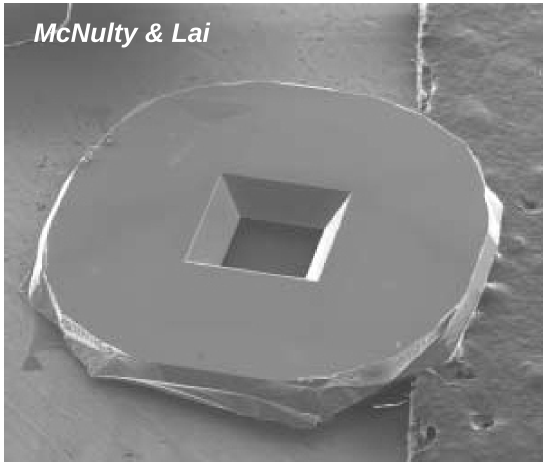

- Need CCD with larger dynamic range
- Perhaps a hybrid direct/lens-coupled CCD
- Finer CCD pixel size

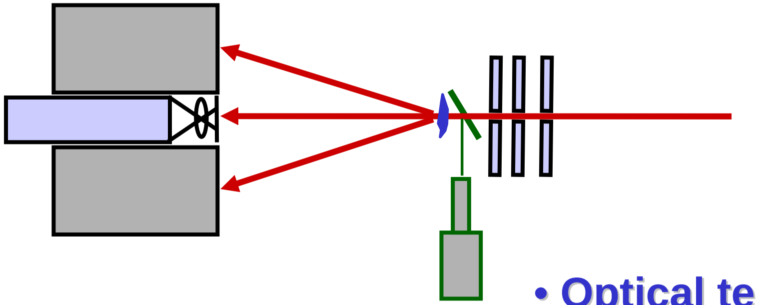

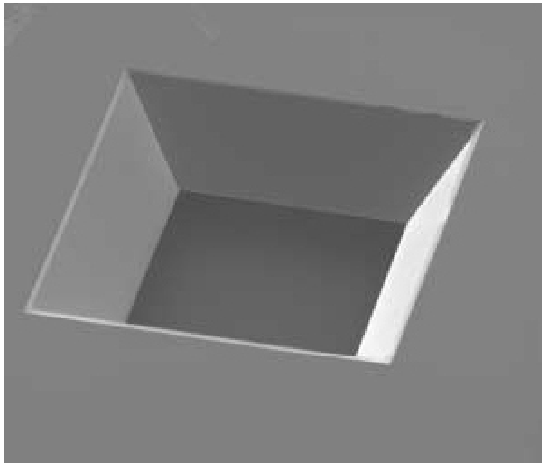

- Optical telescope for sample viewing & centering

Imaging Beamline at Sector 32

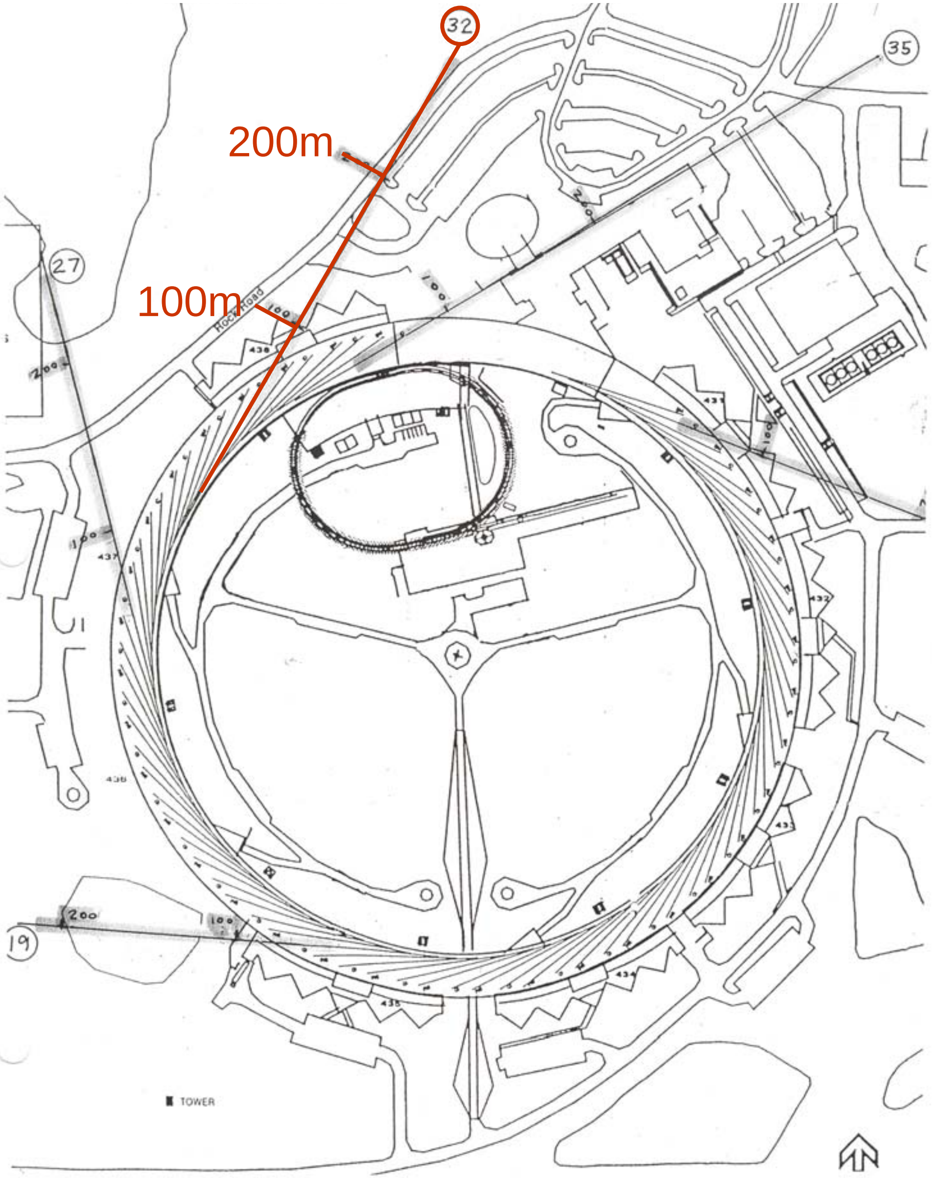

- Consideration of making Sector 32 (Com-CAT) a dedicated imaging XOR-Sector:
  - Phase imaging / tomography
  - Diffraction topography
  - Diffraction enhanced /USAXS imaging
  - Coherent Fresnel diffraction
- Many Benefits:
  - Provides immediate home for the imaging group to satisfy users demand, to expand user base, and to test new application & ideas.
  - Frees up 1-ID so Sector 1 can proceed to become a dedicated high-energy sector.
  - Potential for future expansion perhaps into a long beam line (~200m) with optimized insertion devices.
- Current Status: starting to perform coherent imaging experiments, and to plan for beam line extension.

Proposed Project for a Dedicated Imaging Sector

Phase I: make use of existing hutch and equipment, with upgrades to monochromator & Be windows

→ Phase imaging
→ Diffraction topography
→ USAXS imaging

Phase II: expansion to ~75m by building a new white-beam capable hutch at 75m and beam transport

→ High-sensitivity phase imaging
→ Coherent Fresnel diffraction
→ Projection microscopy

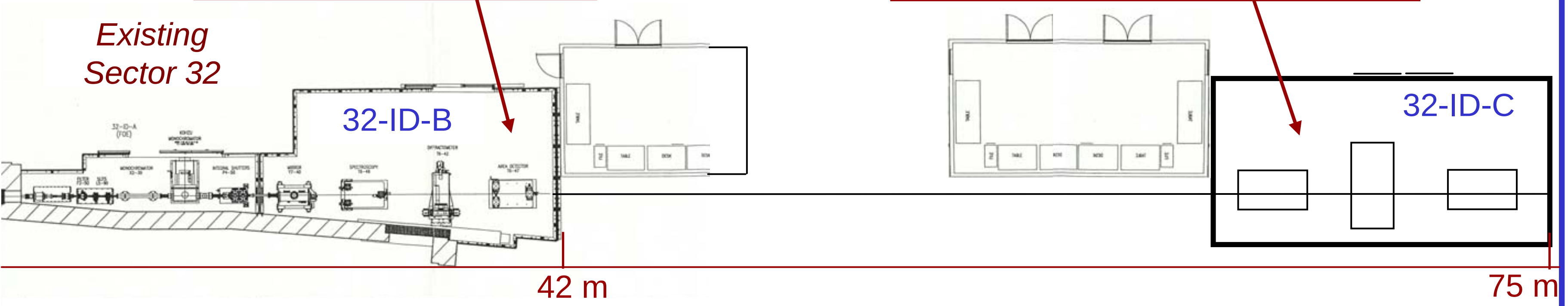

Main Research Programs:

- ***Near-field diffraction and imaging***
- ***Optics development***
- ***Ultrafast imaging with pink beam***

Phase III: future expansion to ~200m (ID-D) with additional outside funding, and with optimized insertion devices and optics

→ Ultra-sensitivity phase imaging
→ Ultra-plane-wave topography
→ Medical imaging ?

Other Applications of Distorted Object

2D Gaussian phase object
➔ Analytical expressions

- ❑ Phase imaging sensitivity study

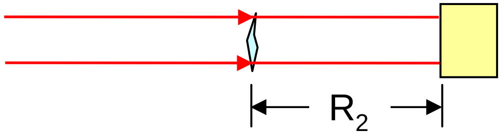

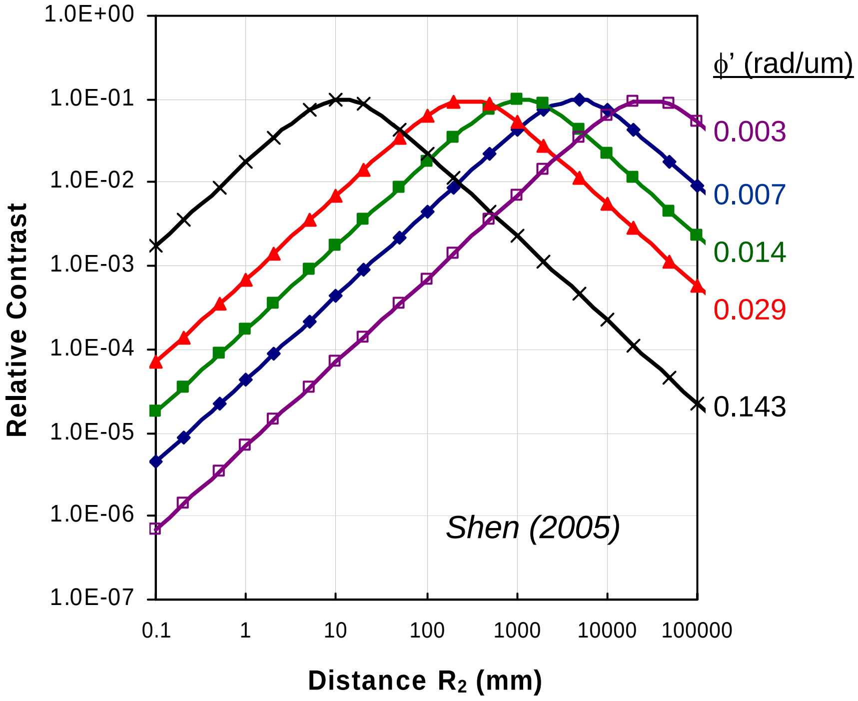

Shen (2005)

- ❑ Coherent diffraction topography

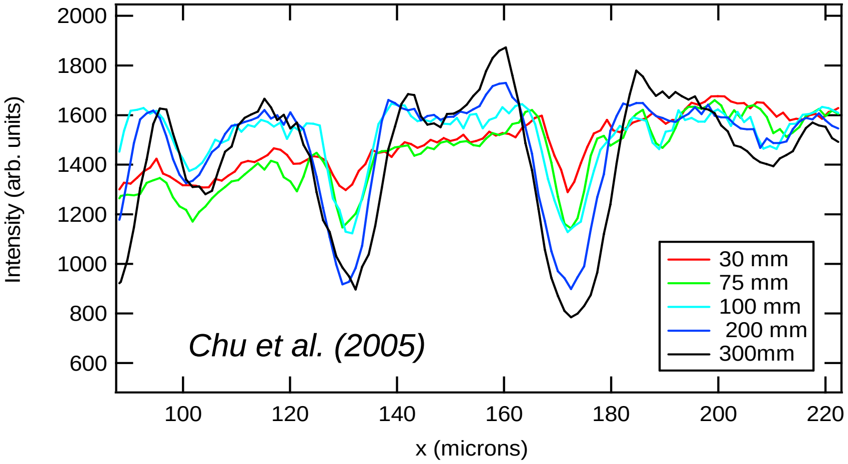

Chu et al. (2005)

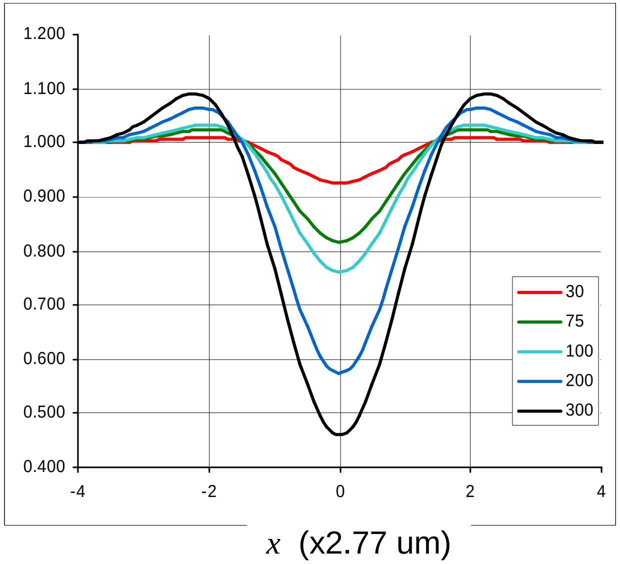

Dose vs. Resolution & Radiation Damage (biomaterials)

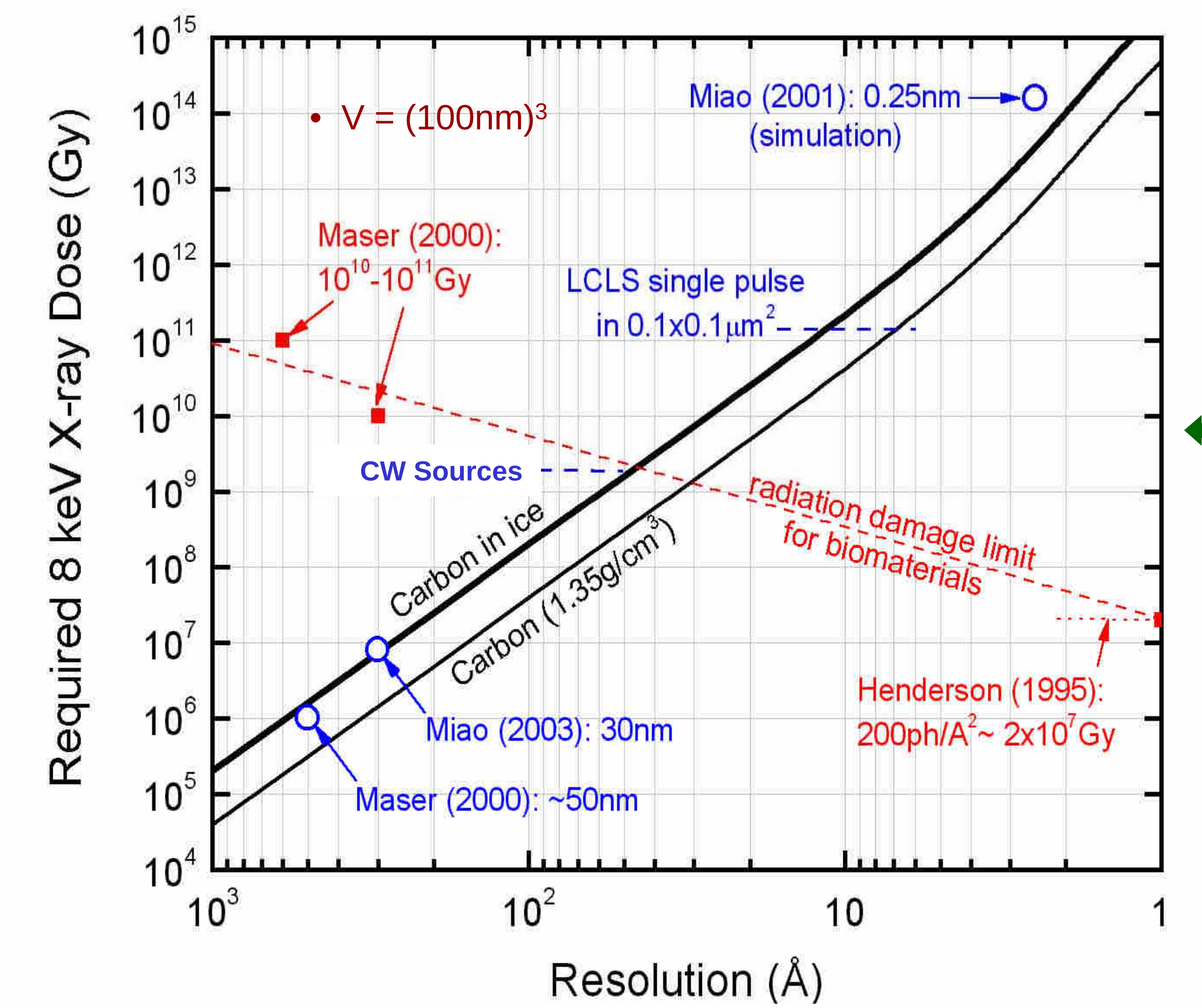

$$Dose = \frac{(I_0\Delta t)\mu \cdot E}{\rho}$$

$$\sim Const.\ in\ \lambda$$

$$(\because I_0\Delta t \sim \lambda^{-2}, \mu \sim \lambda^3, E \sim \lambda^{-1})$$

Shen et al. JSR 11, 432 (2004)

$$\boxed{I \sim L \cdot d^3\lambda^2}$$

L = thickness

Marchesini, Howells, et al. Optics Express (2003)

$$\boxed{I \sim d^4\lambda^2}$$

Summary

- Distorted Object Approach provides a simple universal method for wave field propagation by fast Fourier transform, in both far-field and near-field regimes.
- Distorted Object Approach extends the iterative phasing algorithm to near-field and provides an alternative to far-field coherent diffraction imaging and to astigmatic diffraction with curved beams. It eliminates the Friedel enantiomorph phasing ambiguity in the far-field.
- Practical imaging applications may be in the region where Fresnel number N_z lies between 0.2 – 1, so that requirement on detector pixel size is relaxed but significant Fresnel zone curvature still exists.
- Other applications include design of phase imaging beam line, and phase-sensitive x-ray diffraction topography.
- APS plans to expand in x-ray imaging, including to plan for a bio-nanoprobe beam line, to build a full-field imaging beam line for coherent imaging applications.

Acknowledgments

CHESS (Cornell University):	Xianghui Xiao
X-ray Microscopy Group (APS):	Ian McNulty Zhonghou Cai Yong Chu Stefan Vogt
University of Vermont:	Brad Palmer
X-ray Physics Group (APS):	Peter Lee
Detector Group (APS):	Tim Madden John Lee Steve Ross

Financial support:

Advanced Photon Source is supported by the U.S. Department of Energy, Basic Energy Sciences, Office of Energy Research, under Contract No. W-31-109-Eng-38

CHESS is supported by the U.S. National Science Foundation, under Award No. DMR-0225180.